

PM_{2.5} and gaseous pollutants in New York State during 2005–2016: Spatial variability, temporal trends, and economic influences

Stefania Squizzato^a, Mauro Masiol^a, David Q. Rich^{a,b}, Philip K. Hopke^{a,c,*}

^a Department of Public Health Sciences, University of Rochester School of Medicine and Dentistry, Rochester, NY 14642, United States

^b Department of Environmental Medicine, University of Rochester School of Medicine and Dentistry, Rochester, NY 14642, United States

^c Center for Air Resources Engineering and Science, Clarkson University, Potsdam, NY 13699, United States

ARTICLE INFO

Keywords:

Trends
Air pollution
Spatial variability
Policy
Economics

ABSTRACT

Over the past decades, mitigation strategies have been adopted both by federal and state agencies in the United States (US) to improve air quality. Between 2007 and 2009, the US faced a financial/economic crisis that lowered activity and reduced emissions. At the same time, changes in the prices of coal and natural gas drove a shift in fuels used for electricity generation. Seasonal patterns, diel cycles, spatial gradients, and trends in PM_{2.5} and gaseous pollutants concentrations (NO_x, SO₂, CO and O₃) monitored in New York State (NYS) from 2005 to 2016 were examined. Relationships between ambient concentrations, changes in NYS emissions retrieved from the US EPA trends inventory, and economic indicators were studied. PM_{2.5} and primary gaseous pollutants concentrations decreased across NYS. By 2016, PM_{2.5} and SO₂ attained relatively homogeneous concentrations across the state. PM_{2.5} concentrations decreased significantly at all sites. Similarly, SO₂ concentrations declined at all sites within this period, with the highest slopes observed at the urban sites. Reductions in NO_x emissions likely contributed to summertime average ozone reductions. NO_x and VOCs controls reduced O₃ peak concentrations as seen in significant relationships between the annual O₃ 4th-highest daily maximum 8-h concentrations and estimated NO_x emissions at rural and suburban sites ($r^2 \sim 0.7$). Spring maxima were not reduced with most sites showing insignificant slopes or significant positive slopes (e.g., +2.6% y⁻¹ and +2% y⁻¹, at CCNY and PFI, respectively). Increases in autumn and winter ozone concentrations were found (e.g., $6.6 \pm 0.4\% \text{ y}^{-1}$ on average in New York City). Significant relationships were observed between PM_{2.5}, primary pollutants, and economic indicators. Overall, a decrease in electricity generation with coal, and the simultaneous increase in natural gas consumption for power generation, led to a decrease in PM_{2.5} and gaseous pollutants concentrations.

1. Introduction

It is now recognized that adverse health effects, particularly mortality and morbidity due to cardiovascular and respiratory disease, are associated with increased concentrations of ambient air pollutants (WHO, 2013). Long-term exposure to PM_{2.5} was associated with a 6% and 11% increase in the risk of all-cause and cardiovascular mortality associated with each 10 μg m⁻³ increase in PM_{2.5} concentration, respectively, while each 5.3-ppb increase in NO₂ concentration was associated with a 5% increase in the risk of all-cause of mortality (Hoek et al., 2013). Also, each 10-ppb increase in ambient ozone concentration was associated with an approximate 4% increase in the risk of respiratory mortality (Jerrett et al., 2009). For short-term exposures, Di et al. (2017) determined that an increase of 10 μg m⁻³ in PM_{2.5} and 10 ppb in warm-season ozone were statistically significantly associated

with a relative increase of 1.05% and 0.51% in daily mortality rate, respectively.

During the past forty years, mitigation strategies have been adopted to improve air quality at both the federal and state levels in the United States (US). Since 2000, these strategies were aimed primarily at reducing emissions from light- and heavy-duty vehicles and electric power generation. Between 2004 and 2010, the Tier II Tailpipe NO_x Emissions Standard for light-duty vehicles was implemented (USEPA, 2017a). Major changes included computerized engine control and addition of after treatment technologies. Similarly, the Clean Heavy-Duty Bus and Truck Rule imposed for new heavy-duty diesel vehicles (HDDVs) sold after July 1, 2007, to have particle control traps and after January 1, 2010, to have NO_x controls (USEPA, 2016a). To protect the catalysts in the particle regenerative traps, on-road diesel fuel sold after October 1, 2006, was required to have ultralow sulfur concentrations

* Corresponding author. Department of Public Health Sciences, University of Rochester School of Medicine and Dentistry, Rochester, NY 14642, United States.
E-mail address: phopke@clarkson.edu (P.K. Hopke).

(< 15 ppm) instead of low sulfur content (< 500 ppm) (USEPA, 2016b).

The NO_x SIP (State Implementation Plan) Call finalized in 2004 and the NO_x Budget Trading Program (2003) strongly reduced summertime NO_x emissions from power plants and other large stationary sources (USEPA, 2017b). It was estimated that the NO_x SIP call led to a 57% reduction in NO_x emissions from 2000 to 2005 (Simon et al., 2015). In 2003, a new regulation on electricity generated emissions of SO₂ and NO_x started in New York State (NYS) (NYSERDA, 2006). The regulation required New York electricity generators to reduce SO₂ emissions by 50% below levels allowed under the Clean Air Act. It also extends the NO_x emissions limits currently required for the ozone season throughout the year. In 2004, the Renewable Portfolio Standard, approved by the NYS Public Service Commission, aimed to include a higher proportion of renewable energy sources in the state electricity generation mix, such as wind power and other “green” alternatives to fossil fuels from 19% to more than 25% by 2013. A potential reduction in ozone precursors (NO_x and CO) and PM can be also associated with the introduction of the Regional Greenhouse Gas Initiative (RGGI) in 2009 (NYSERDA, 2006). This multi-state effort aimed to cap carbon dioxide emissions associated with the generation of electricity in the Northeast and mid-Atlantic US. RGGI includes investments in energy efficiency, clean and renewable energy, and greenhouse gas abatement mostly addressed to the residential and business recipient. This program led to a reduction in power sector carbon pollution of more than 45 percent (RGGI, 2017). In New York City in 2011, new permits for No. 6 oil used for space heating were disallowed so that by 2015, only No. 4 or cleaner oil could be used. However, No. 4 oil could still contain 1500 ppm S (Kheirbek et al., 2014). NYC Cleanheat (2018) claims a 65% reduction in PM_{2.5} emissions from building heating because of switching to cleaner fuels.

Beginning on July 1, 2012, NYS required that all distillate oils including No. 2 oil sold within the state for any purpose be ultralow sulfur. This requirement has been adopted by most northeastern states in 2014 (NEFI, 2014). In addition, there have also been reductions in emissions from upwind sources that provide the precursor gases for particulate sulfate and nitrate (SO₂ and NO₂) including electricity policy changes in Ontario, Canada (CA) that phased out all fossil fuel combustion for electricity generation (Ontario, 2017).

Previous air pollution long-term trend analyses in Rochester, NY (Emami et al., 2018) showed significant declines in concentrations for most air pollutants at single locations. Duncan et al. (2016) reported notable drops in urban NO_x over the northeastern US from 2005 to 2014. However, the eastern US is still affected by the highest mass concentrations of airborne fine particulate matter (PM_{2.5}) in the US (Fine et al., 2008; Hand et al., 2012a, 2012b; Tai et al., 2010) and SO₂ emissions are higher than the western US leading to a larger contribution of ammonium sulfate on PM mass (Parrish et al., 2011).

Recently, Rattigan et al. (2016) examined trends in concentrations of PM_{2.5} and its major constituents at 8 sites in NYS. They reported reductions of 4–7 μg m⁻³ at urban sites compared with 3–4 μg m⁻³ for rural locations between 2000 and 2015. They attributed much of these reductions to lower sulfate and nitrate concentrations. Giverolo et al. (2017) analyzed the 1980–2014 trends of the annual averages of gas-phase pollutants as well as seasonal and diurnal variations at 5 urban and one rural sites to evaluate the impacts of the emissions control programs. However, there has not been an analysis of the spatial distribution and pollutant concentration variations across NYS. The relationships between pollutant concentration trends, national emission estimates, and whether any pollutant concentration changes driven by changing economic conditions (e.g., the 2008 recession) have not yet been explored. Moreover, although most of NYS's population lives in urban areas, the state is also characterized by small villages across the state. Hence, a complete analysis of trends in pollutant concentrations acquired at all of the urban, suburban, and rural sites is needed.

In this study, PM_{2.5} and gaseous pollutants concentrations (NO_x,

SO₂, CO and O₃) monitored by the New York State Department of Conservation (DEC) from 2005 to 2016 were analyzed to determine the seasonality, diel cycles, spatial gradients, and trends across NYS. Changes in emission rates for NYS retrieved from the US EPA trends inventory database were related to the ambient pollutants concentrations, and the effect of economic changes on these trends were also assessed using a variety of economic indicators.

2. Study area and emissions scenario

2.1. Study area

NYS extends over 141,000 km² (max extension ~500 km along its N-S axis and ~520 km along its W-E axis). Its territory includes several major metropolitan areas (≥1 million inhabitants: New York City, Buffalo, Rochester, and Albany) and many smaller urban areas, to give a total population of ~19.7 million inhabitants (Census, 2017a). According to the 2011 National Land Cover Database, ~8.3% of the NYS territory is developed areas (Homer et al., 2015). However, most of the land area (58.5%) hosts natural and semirural environments (barren land, forest, shrub, grassland and wetland), pasture/hay, and cultivated crop (19.2%) and water bodies (13.7%). In addition to local emissions, air quality in NYS is affected by transported air masses from other source areas, such as the Ohio River Valley (Dutkiewicz et al., 2011; Masiol et al., 2017a; Emami et al., 2018).

Seven metropolitan combined statistical areas were classified in NYS in 2013 (Census, 2017b): (i) Albany-Schenectady (population 1.2 million); (ii) Buffalo-Cheektowaga (1.2 million); (iii) Elmira-Corning (183,000); (iv) Ithaca-Cortland (153,000); (v) Rochester-Batavia-Seneca Falls (1.2 million); (vi) Syracuse-Auburn (743,000) and (vii) New York City (NY-NJ-PA Metro Area, 23.7 million).

2.2. Changing in emissions

Air pollutants emission inventory trends data for NYS are available from the US EPA trends inventory for the 1990–2016 period (USEPA, 2017c). Some technical specifications about the US EPA trends inventory are reported in supplemental section S1. The trends for the total emissions of primary PM_{2.5} and the main gaseous precursors for secondary PM (SO₂, NO_x, NH₃, and VOCs), at state-level, for the period 2005–2016 are provided in the supplementary material (Section S1 and Figs. S1 to S6).

PM_{2.5} is emitted mainly by three sectors: “fuel combustion other”, which includes different combustion processes (boilers, engines) and different fuels (coal, kerosene, distillate oil, residual oil, wood); “miscellaneous sources” including emissions from aircraft, paved road, unpaved road, construction and agriculture; and “other industrial processes” including commercial cooking, grain mills, feed mills, stone quarrying/processing, mining, etc. Total PM_{2.5} emissions showed an increase since 2012, mostly attributable to the increase in the estimated emissions from the “other industrial process” sector due to changes in emission estimates for commercial cooking.

NO_x and SO₂ emissions have decreased by 52% and 85%, respectively, mostly associated with the decrease in the emissions from highway and off-highway vehicles and fuel combustion for electric power generation. Similarly, VOC and CO emissions decreased sharply (–60% and –45%, respectively). Highway and off-highway vehicles are the main sectors emitting both VOCs and CO. VOC emissions are also attributed to changes in solvent utilization.

While most emissions reductions can be ascribed to regulations and associated technological improvements, economic drivers can also affect emissions and resulting ambient concentrations of air pollutants as well as the composition of particulate matter (Arruti et al., 2011). To better understand the economic variations occurring in the 2005 to 2016 period, the net generation of electricity by energy source, the energy sales by sector, and the residential oil and gasoline prices were

reviewed. Net electricity generation by energy sources in the US and NYS is presented in Figs. S7 and S8. At the national level, there was a rising trend in net electricity generation until 2009, followed by level production. In NYS, electricity generation decreased between 2007 and 2009 and then remained constant.

In 2008 and 2009, coal used for power generation started to decline and natural gas increased both at the state and national level because of changes in the operating costs driven by the relative costs of these fuels (Fig. S9). The effects of the 2008 financial crisis (started in October 2007) are reflected in energy sales for the industrial sector (Fig. S10) and the transportation sector (Fig. S11), with decreased energy sales at the end of 2007 until 2012. Furthermore, by 2010, escalating and highly variable prices for electricity, natural gas, and residential oil (Fig. S12) led to an increase in the NYS market share for wood. Wood was used to supplement oil, gas, propane, and electricity particularly in low-income households when temperatures were low or fuel prices were high (Loughlin and Dodder, 2014) and in areas without a ready access to natural gas (NYSERDA, 2016).

3. Material and methods

3.1. Air pollution data

PM_{2.5} and gaseous pollutants concentrations (SO₂, O₃, CO and NO_x) were retrieved from US EPA (<https://aqs.epa.gov/api>). Measurements were made using the current and past FEMs (federal equivalent methods) and FRMs (federal reference methods) (DEC, 2017; Civerolo et al., 2017). Only the sites collecting PM_{2.5} by the federal reference method (FRM) (i.e., gravimetric determination) were considered. In 2015, the NYS Department of Environmental Conservation (DEC) managed 74 sites and additional sites were managed by the US EPA - Clean Air Markets Division and by tribal agencies. The sites having at least 6 years of data for at least one pollutant during the period 2005–2016 were included in this study. The final dataset included data from 54 sites (26 for PM_{2.5}, 37 for O₃, 26 for SO₂, 8 for NO_x, 2 for NO_y, 11 for CO) categorized as urban and center city (URB = 17), suburban (SUB = 15), and rural (RUR = 22). The specific sites, their locations, owners, site abbreviation, category, and species measured are listed in Table S1. Five main spatial categorizations were identified on the basis of US EPA core based statistical areas (CBSA): (i) Buffalo, also including the Cheektowaga and Niagara Falls area; (ii) Rochester-Syracuse-Utica including the Rome, Ithaca, Syracuse and Corning areas; (iii) Upstate NY including rural sites located in the Northern part of the state; (iv) Albany, including the Kingston and Albany-Schenectady-Troy areas; and (v) New York City (NYC), which groups the sites of the New York-Newark-Jersey City area. A map of the sites is provided in Fig. 1.

Preliminary data handling and clean-up were performed to check the datasets for robustness, outliers, and anomalous records. Data below the detection limit (DL) were replaced with DL/2. Data were adjusted to account for the shift in anthropogenic emissions due to the changes between local time and daylight savings time (DST) as needed. This latter correction helps in investigating diel patterns of anthropogenic emissions.

3.2. Data analyses

Data were analyzed using R (R Core Team, 2017) and a series of supplementary packages, including ‘openair’ (Carslaw and Ropkins, 2012; Carslaw, 2017), ‘corrplot’ (Wei et al., 2017) and ‘gstat’ (Pebesma and Graeler, 2017). Theil-Sen slope estimation coupled with the non-parametric Mann-Kendall analysis was used to analyze trends in those sites having at least 9 years of data (Sen, 1968; Theil, 1992). This technique assumes monotonic linear trends and is therefore useful to estimate the interannual trends. The slopes were also deseasonalized by using the seasonal trend decomposition using loess (STL) to exclude the effect of seasonal cycles. Long-term trends were analyzed using the

monthly-averaged data between 2005 and 2016, with only those months having at least 75% of possible measured concentrations included in the analysis.

Inverse distance weighting (IDW) was applied for spatial interpolation of the pollutants distributions using the seasonal averages as input data. This technique has been previously applied in exposure assessment studies (e.g., Hystad et al., 2011; Wu et al., 2006; Masiol et al., 2016) to generate pollutant concentration surfaces. IDW assumes that each measured point has a local influence that diminishes with distance giving greater weights to points closest to the prediction location. Using IDW, the influence of neighboring points is lowered as a function of the increasing distance d (d^2 in this case). This implies that the spatial interpolation can reflect a localized or a more extended condition based on the spatial scales of representativeness of the measured points. Tables S2 to S4 report the measurement scale for each sampling sites following the US EPA classification. Ozone monitoring sites are mostly classified as representative of urban and regional conditions (4 km–50 km and 50 km to hundreds km of spatial representativeness, respectively). For PM_{2.5} and SO₂, sampling sites are mostly representative of a neighborhood scale (100 m–4 km) increasing the uncertainty associated to the spatial interpolation in areas with low-points density (e.g., the northern part of the NYS).

To better cover the entire state, particularly along its borders, pollutant concentration data from the adjacent sites in Pennsylvania, New Jersey, Vermont, and Ontario (Canada) were also included (Table S5). Data for the Ontario sites were retrieved from the National Air Pollution Surveillance Program website (NAPS, 2017).

4. Results and discussion

4.1. Average concentrations, seasonal variation and diel patterns

Fig. S13 shows a summary of the data distributions for the whole study period (all available data). Concentrations are expressed as indicated by the NAAQS: ppb for NO_x and SO₂, ppm for O₃ and CO, $\mu\text{g m}^{-3}$ for PM_{2.5}. Month of the year and diel patterns (except for PM_{2.5}) are shown in Figs. 2–4, while day of week patterns are shown in the supplementary material (Figs. S14 to S16).

4.1.1. Ozone

During the whole period, the highest average ozone concentrations were observed at CON, WES, RIV and WHF (0.035 ppm), DUN (0.033 ppm), and AMH (0.030 ppm). Different monthly patterns were observed as a function of the state region and sampling site categorization:

- Buffalo area sites (AMH and DUN) showed the high, stable concentrations during April through July. The lowest average concentrations were reached in December and January, but were still higher compared to the other sites in the same months (O₃ > 0.020 ppm).
- NYC area sites (CCNY, IS52, QUE, PFI, BAB, HOL, WHP, SUS and RIV) showed two distinct peaks: one in April (O₃ ~ 0.030 ppm) and one in July (O₃ ~ 0.035 ppm)
- Similar to the rural sites, ROC, SYR, VAL, and LOU exhibited the highest concentrations in April and May (O₃ ~ 0.035 ppm) and a minimum during the coldest months with O₃ average concentrations (O₃ ~ 0.020 ppm) comparable to the rural sites (MID, MIL, MTN, NIC, PIN, WHF, WIL, ROCK, PIS, PER).

The seasonal ozone cycle shows distinct maxima during spring at some rural locations that are less affected by anthropogenic emissions and the magnitudes of the maxima have increased (Monks, 2000; Chan and Vet, 2010; Austin et al., 2015). Spring maxima could be related both to the stratosphere-troposphere exchange (STE) of O₃-rich stratospheric air into the troposphere and to decomposition of NO_x reservoirs

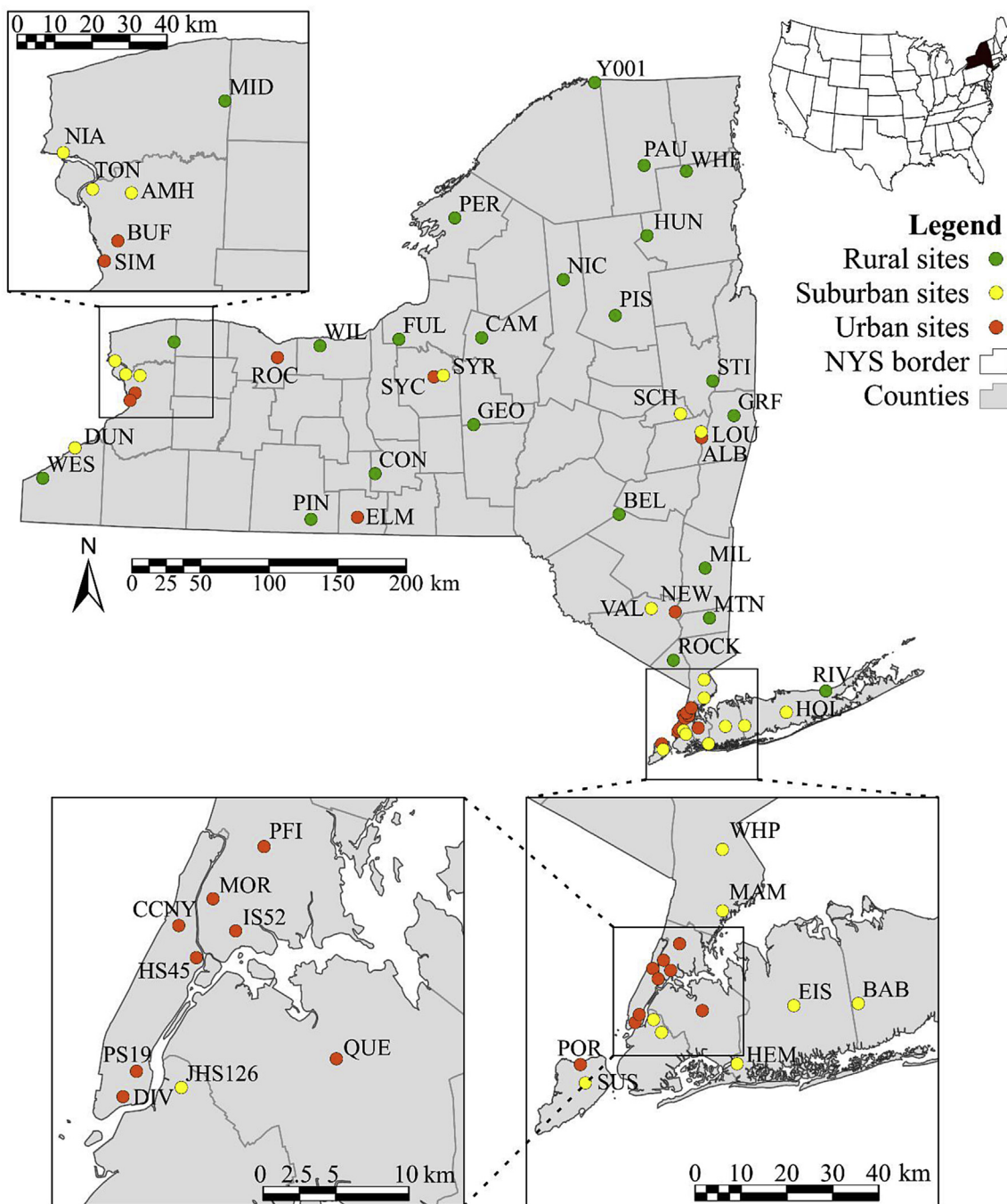


Fig. 1. Sampling sites.

such as PAN accumulated during the winter (Bloomer et al., 2010; Clifton et al., 2014; Gao et al., 2013; Parrish et al., 2013; Strode et al., 2015; Vingarzan, 2004). However, there is no consensus as to the origin of the spring maximum (Vingarzan, 2004). Both of these effects will occur, but the relative role of each at any given location and time is not known.

Across the state, ozone presented a diel pattern with the highest concentrations during the afternoon, i.e. the hours characterized by the higher solar radiation, and minimum concentrations at 6–7 a.m. During the week, the highest concentrations were reached during weekend days (Saturday and Sunday) at urban and suburban sites (Cleveland et al., 1974; Lebron, 1975; Cleveland and McRae, 1978) when the lowest concentrations of NO and NO₂ are also recorded. Rural sites exhibited a flattened weekly pattern that can be related to the lack of

anthropogenic ozone-precursors and the higher availability of the biogenic VOCs.

A total of 1681 exceedances of the 8 h national ambient air quality standard (NAAQS) implemented in 2015 (0.070 ppm) were recorded across the state, mostly during the period 2007–2012. At some sites, a strong decrease in the number of exceedances was recorded (i.e., HOL, n = 41 in 2007, n = 6 in 2011; DUN, n = 29 in 2007, n = 1 in 2013). Despite this decline, the 8 h-standard was exceeded 101 times in 2016, mostly in the NYC and surrounding areas (USEPA, 2017d).

4.1.2. Nitrogen oxides

NO_x is generally used as a marker for combustion emissions, particularly from road traffic. The highest annual average NO_x, NO, and NO₂ concentrations were observed at the NYC sites, with NO_x ranging from

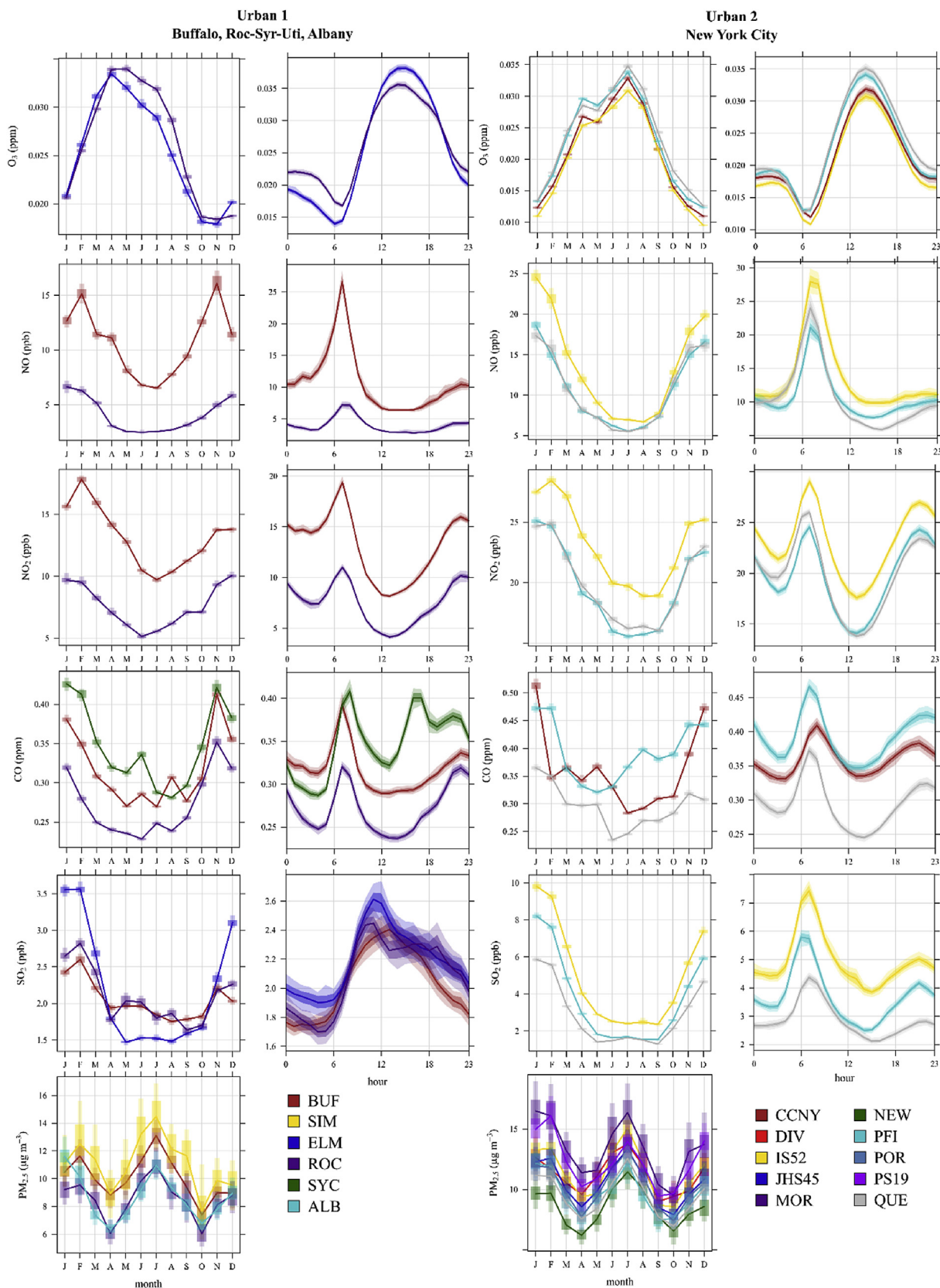


Fig. 2. Seasonal and diel variations of the monitored pollutants at urban sites. Each plot reports the monthly average and the hourly average concentrations as a filled line and the associated 75th and 99th confidence intervals calculated by bootstrapping the data (n = 200).

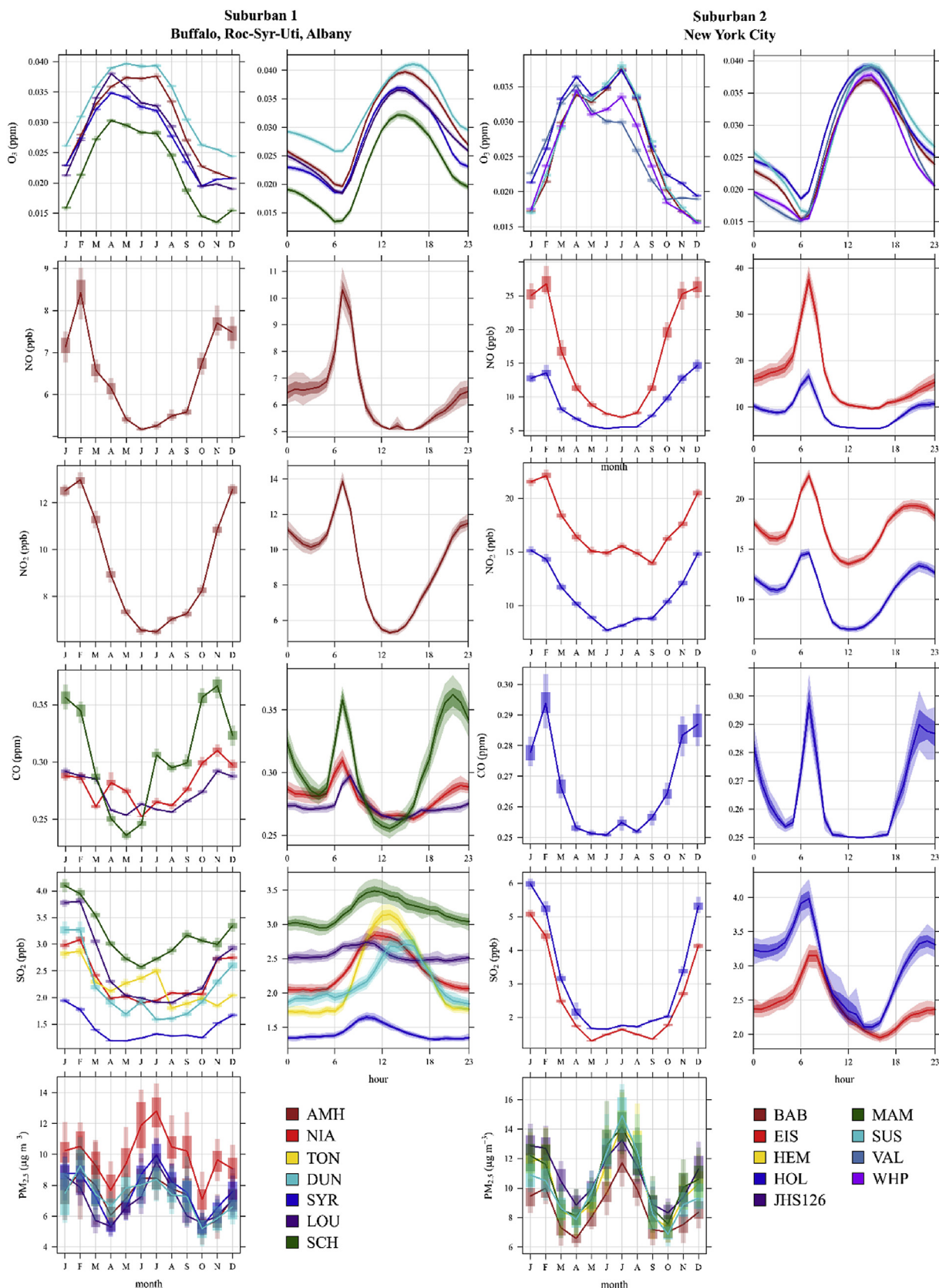


Fig. 3. Seasonal and diel variations of the monitored pollutants at suburban sites. Each plot reports the monthly average and the hourly average concentrations as a filled line and the associated 75th and 99th confidence intervals calculated by bootstrapping the data (n = 200).

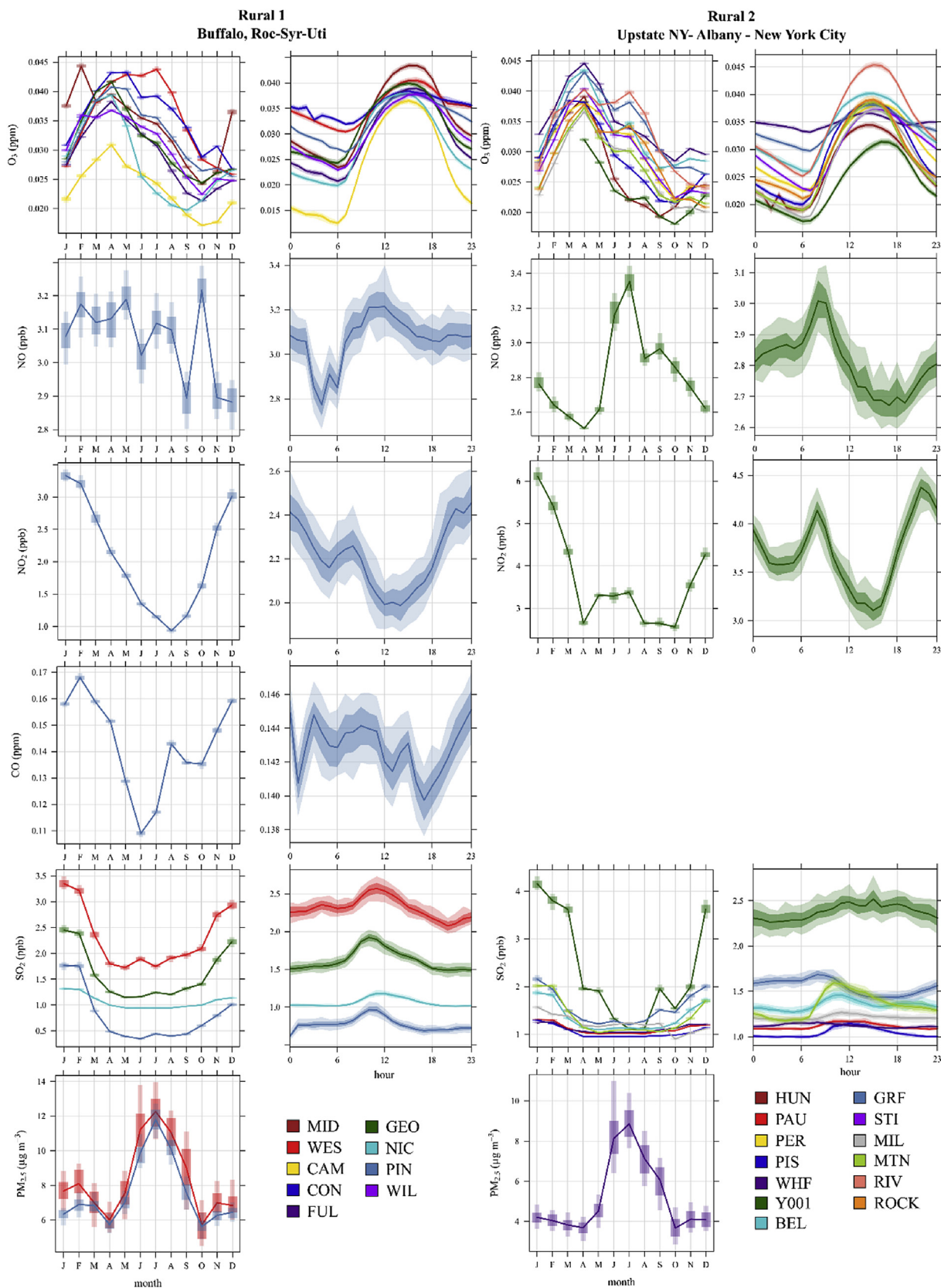


Fig. 4. Seasonal and diel variations of the monitored pollutants at rural sites. Each plot reports the monthly average and the hourly average concentrations as a filled line and the associated 75th and 99th confidence intervals calculated by bootstrapping the data (n = 200).

35 ppb at IS52 to 28 ppb at PFI. Among the other urban sites, ROC had the lowest average concentration (11 ppb) while the rural minima were observed at Y001 (4 ppb) and PIN (2 ppb). At urban and suburban sites, nitrogen oxides showed the highest concentrations during the cold months and the lowest during the warm ones. This pattern can be attributed to the increase in combustion for space heating, lower mixing layer heights, lower wind speeds, and the reduced availability of oxidant species (hydroxyl radical and ozone).

Two diel NO₂ peaks were found at urban and suburban sites, one in the morning between 7 and 8 and one in the evening. NO showed a morning peak similar to NO₂ but with a smaller increase during the evening because of the higher afternoon ozone concentrations as noted above. Diurnal variation in road traffic emission and mixing layer height can explain this pattern with the midday minimum associated with lower traffic emissions, higher ozone concentrations, and a deeper mixed layer with higher wind speeds enhancing atmospheric mixing. Weekly mean values were quite similar from Mondays to Friday followed by a drop in average concentrations during the weekend (Saturday–Sunday). The decrease in concentrations at the end of the week can be attributed to lower traffic volumes compared to the other days. Traffic data was retrieved by the New York State Department of Transportation (NYSDOT, 2017); the closest traffic count site was chosen for each site. Examples of weekly traffic volume patterns for IS52, PFI, QUE, HOL, BUF, AMH, PIN, Y001 and ROC is presented in Fig. S17.

4.1.3. Carbon monoxide CO

Similar to other pollutants, the highest average concentrations of CO were recorded at the NYC sites (CCNY and PFI, 0.39 and 0.36 ppm, respectively) whereas the minimum was reached at PIN (0.14 ppm). Monthly, weekly and diel concentration patterns are like those observed for NO_x. Cold months had the highest average concentrations and decreased concentrations on the weekends. Two diel peaks were observed: one in the morning (7–8) and one in the evening at all sites except PIN, thereby relating CO concentrations to traffic emissions.

4.1.4. Sulfur dioxide

The highest average SO₂ concentrations were recorded in the urban and suburban sites. NYC area had the highest concentrations (IS52, 5.0 ppb; PFI, 3.7 ppb; SCH, 3.2 ppb; HOL, 3.0 ppb; QUE, 2.9) compared to Buffalo (WES, 2.3 ppb; TON, DUN 2.2 ppb; BUF, 2.0 ppb), Rochester-Syracuse-Utica (ROC, 2.1 ppb; ELM, 2.2 ppb; SYR, 1.4 ppb) and the rural sites (~1 ppb) except for Y001 (2.4 ppb). At the NYC sites, LOU, and rural PIN and MTN, SO₂ monthly average concentrations exhibited a typical pattern with the highest concentration during the colder month and the lowest concentrations during the summer. This NYC pattern can be ascribed to the use of residual oil for space heating. Masiol et al. (2017a) reported increased probabilities of high SO₂ concentrations when winds blew from Manhattan toward Queens. Lower mixing layer heights, lower wind speeds, and possible thermal inversions limit dispersion and trap the local emitted pollutants close to the ground. At BUF, DUN, ROC, SYR and the rural sites other than PIN and MTN, the SO₂ concentrations were slightly higher in the coldest month, but the differences between summer and winter were less. Summer increases in SO₂ might be related to the use of peaking diesel generators to satisfy the higher power demand for air conditioning. The diesel generators would use nonroad fuels that would be higher in S content prior to 2014 resulting in higher SO₂ emissions.

No specific weekly pattern can be identified, but there is a marked diel pattern. In NYC, the diel pattern is characterized by two peaks in concentrations, one in the early morning (~6–7) and one in the evening (~21–22), compatible with the emissions related to space heating and traffic. Other sites (SYR, LOU, ROC and RUR sites) showed an increase during late morning (~10–11). TON, DUN and BUF exhibited an unusual pattern, with the SO₂ maxima during the afternoon (~12–16). This pattern was related to industrial emissions (Emami et al., 2018).

During daytime, the rising mixing layer allows the intrusion of polluted air masses aloft from farther areas to downmix, resulting in increased concentrations. A similar daytime increase was also reported by Masiol et al. (2017c) and Bigi and Harrison (2010). These increases were also attributed to downward mixing of plumes from elevated point sources as the boundary layer deepens during daylight hours.

4.1.5. Particulate matter PM_{2.5}

Statewide, New York City had the highest average PM_{2.5} concentration. For the whole period, MOR, PS19, and IS52 showed annual average concentrations of 13.3, 12.2, and 11.4 μg m⁻³, respectively. Lower concentrations were observed at all rural and suburban sites. WHI showed the lowest annual average PM_{2.5} concentration (5.2 μg m⁻³) whereas PIN and WES had average concentrations comparable to suburban sites (PIN 7.6 μg m⁻³, WES 8.3 μg m⁻³, AMH 7.2 μg m⁻³, DUN 7.2 μg m⁻³, SYR 7.5 μg m⁻³).

Common seasonal patterns were detected across the state showing the highest average concentrations during summer months with RUR sites (PIN and WHI) reaching similar PM_{2.5} concentrations to suburban and urban areas. Urban and suburban areas also showed an increase in concentration during cold months, with similar concentrations to the summer period at some sites (i.e., BUF, ALB, DIV, IS52, and JHS126). During winter, the lower mixing layer height including thermal inversions, and the higher pollutant emissions due to space heating produced increased PM concentrations. During summer, enhanced photochemical activity increased the formation of ammonium sulfate and secondary organic aerosol (SOA) that are the major PM_{2.5} constituents in the northeastern US (Malm et al., 2004; Fine et al., 2008; Tai et al., 2010; Masiol et al., 2017b).

4.2. Intersite correlations

The coefficients of determinations (r²) were calculated to evaluate the site-to-site correlations. The correlation plots for PM_{2.5} and O₃ for the entire period and each season are shown in Figs. S18 to S22. The highest correlations for PM_{2.5} concentrations were observed within the NYC, Albany, Buffalo, and Rochester areas. ALB, LOU (located in the central part of the state) and NEW (north of New York City) provided different results, showing high r² values with the New York City sites and with the Buffalo and Rochester sites suggesting the influence of regional PM.

The PM_{2.5} intra-group correlation (r² > 0.7) as well as the inter-group correlations between the northern and the central sites and the central and NYC sites were generally high (r² > 0.5) (Fig. S18). PM_{2.5} variations can be attributed both to local and regional processes. The influence of regional processes on sulfate was described by Dutkiewicz et al. (2004). They reported that sulfate showed similar concentrations and trends across the state, and PM_{2.5} concentrations were well correlated even for sites separated by 350–390 km and representing highly varying local environments (QUE, PIN and WHF).

Compared to PM_{2.5}, ozone showed a more heterogeneous spatial pattern, with lower inter-site correlations (Fig. S19). The highest correlations can be observed within the NYC sites, and generally between neighboring sites (i.e., ROC and AMH, MTN and VAL, STI and LOU) without any distinction based on site categorization (urban, suburban and rural). Summer period (June–July–August) exhibited an increase in similarity and slightly higher r² (Fig. S20).

SO₂ concentrations were highly correlated among the NYC sites (EIS, IS52, PFI, and QUE) (r² > 0.6) (Fig. S21). The other sites generally exhibited lower r² values, suggesting the presence of specific SO₂ sources driving local SO₂ temporal variation.

Like SO₂, nitrogen oxides, total reactive nitrogen and carbon monoxide did not show regional or area-specific characteristics (Fig. S22). For NO_x and NO_y the highest r² can be observed between the NYC sites (QUE, IS52, PFI, HOL, and EIS) and between AMH and BUF (r² = 0.5). However, these pollutants were only monitored at a few sites that not

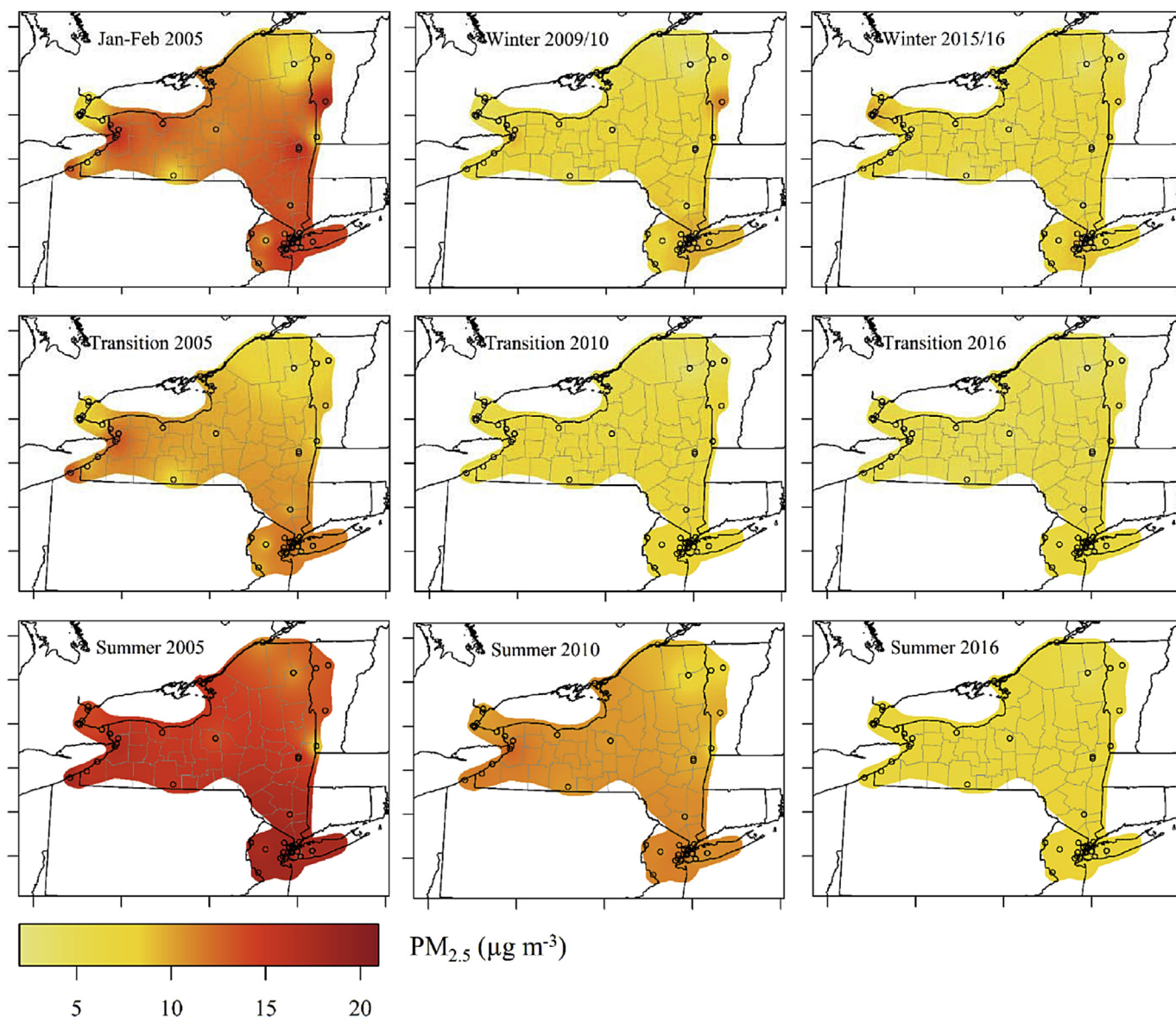


Fig. 5. Spatial interpolation of $PM_{2.5}$ concentrations.

allow for good spatial characterization.

4.3. Spatial distribution

Spatial differences in anthropogenic sources as well as the topographic features, can influence the pollutants distribution across the state. To better highlight the most polluted areas and the changes in pollutants concentration over the 2005–2016 period, seasonal average concentrations of $PM_{2.5}$, O_3 and SO_2 were interpolated by using an inverse distance weighted (IDW) power 2 technique to generate maps for each season along the investigated period.

Three seasonal periods were considered for $PM_{2.5}$ and SO_2 , based on the seasonal patterns: winter (Dec–Jan–Feb), summer (Jun–Jul–Aug) and transition (Mar–Apr–May–Sep–Oct–Nov). Ozone concentrations were investigated over the four seasons because of the spring maxima observed and the different patterns exhibited at the rural, suburban and urban sites: spring (Mar–Apr–May), summer (Jun–Jul–Aug), autumn (Sep–Oct–Nov) and winter (Dec–Jan–Feb). Carbon monoxide and nitrogen oxides were not considered because of the limited number of sites (11 sites and 10 sites, respectively). Seasonal maps for 2005, 2010 and 2016 are presented in Figs. 5–7. Animated figures showing the variation of years

for each pollutant for each season are available as separate supplementary material files.

$PM_{2.5}$ showed the highest concentrations in the metropolitan areas during summer months (Fig. 5). Average concentrations increased from north to south reaching the maxima in NYC. In winter, $PM_{2.5}$ concentrations reached a virtually identical spatial distribution between NYC, Albany, Rochester and Buffalo. A gradual reduction in $PM_{2.5}$ concentrations occurred across the state that was most evident in summer. The result of this decrease is a homogeneous $PM_{2.5}$ distribution across the state.

Ozone exhibited different patterns (Fig. 6). Summer months showed a decrease in ozone concentrations, mostly in the central and north part of the state what ozone increased during winter and spring leading to a less spatial variability. During spring 2016, the Pinnacle–Connecticut Hill area and Whiteface still represented ozone hotspots, but the concentrations across the state were similar with the lowest average concentrations in New York City. During winter, the increasing time trend is evident with most of the urban and suburban sites reaching similar concentrations as some of the rural sites, mostly associated with the increase of ozone average concentration in the metropolitan areas than decreases at the rural sites. The increases in winter ozone are attributed

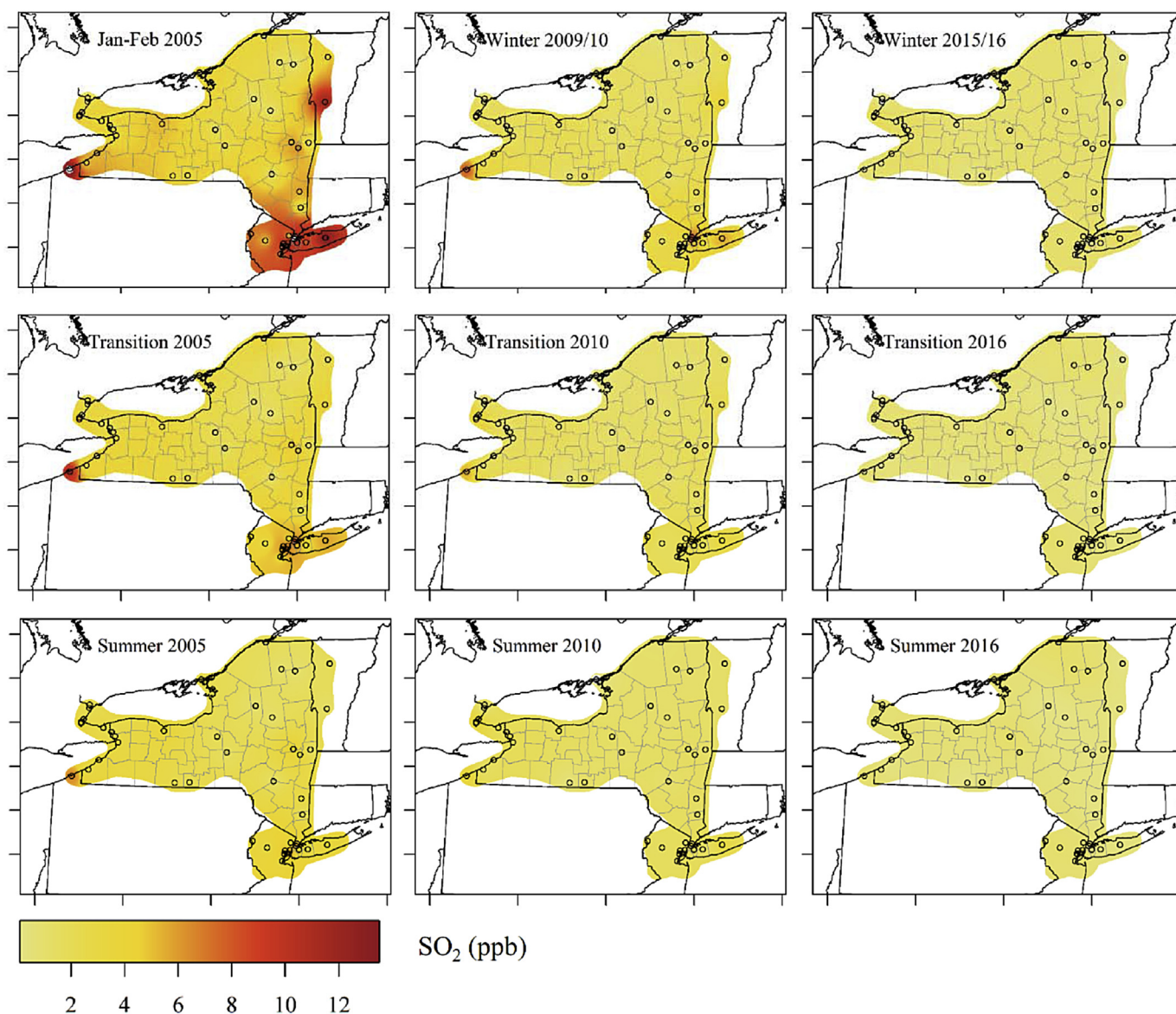


Fig. 6. Spatial interpolation of SO₂ concentrations.

to the declines in NO_x emissions (Clifton et al., 2014).

SO₂ concentrations exhibited a strong decrease across the state (Fig. 7). While the decrease is rather homogeneous across the state, highlighting the presence of common sources of SO₂ at all sites, IS52 and PFI located in the Bronx area (NYC) showed a different time pattern. During 2005–2011, the drop in SO₂ concentrations at IS52 and PFI were smaller than at the other sites. In 2012, these sites remained hotspots. From 2013 onwards, the decrease in concentration was more evident and very low concentration were observed in 2016 also at IS52 and PFI. This behavior was likely due to the effect of the introduction of ultralow-sulfur residential oil regulation for space heating in New York State.

4.4. Trends analysis

Table 1 provides the Theil-Sen linear slopes as percentage y⁻¹ during the period. Trend analysis was also applied to monthly averages for each pollutant by season to better characterize the effect of the control strategies. These results are reported in Tables S6 to S9. Hidy et al. (2014) suggested regressing the annual average ambient concentrations for each pollutant on the annual total state-level estimated

emissions of SO₂, NO_x, CO and VOCs. Examples of these results are presented in Fig. 8 with complete results presented in Table S10.

PM_{2.5} concentrations decreased significantly (*p*-value < 0.05) at all sites with slopes ranging from $-8.6\% \text{ y}^{-1}$ at POR and JHS45 and $-2.2\% \text{ y}^{-1}$ at PFI. Seasonally, the highest statistically significant slopes were observed during summer at almost all sites with an average decrease of $-5 \pm 0.6\% \text{ y}^{-1}$. During the winter and transition seasons, the estimated slopes showed smaller decrements except at SYR, BUF and ALB showing concentrations decreases similar to the summer period ($-4.2\% \text{ y}^{-1}$ and $-4.4\% \text{ y}^{-1}$ in winter and summer, respectively). The larger decrease during the summer months is consistent with the decrease in sulfate concentrations observed in New York State (Rattigan et al., 2016) and in the Eastern US (Malm et al., 2002). This decrease reflects both the regional origins of the sulfate particles and the overall effect of the reduction of SO₂ emission from electric generating utilities (EGUs) in high emitting areas such as the Ohio River Valley and the Great Lakes Basin (Dutkiewicz et al., 2004).

Significant negative trends in NO_x were observed, ranging from $-0.4\% \text{ y}^{-1}$ at BUF to $-4.2\% \text{ y}^{-1}$ at QUE. However, no significant trend was found at PIN. The observed trends are consistent with the decreases in NO_x emissions in NYS resulting in statistically significant

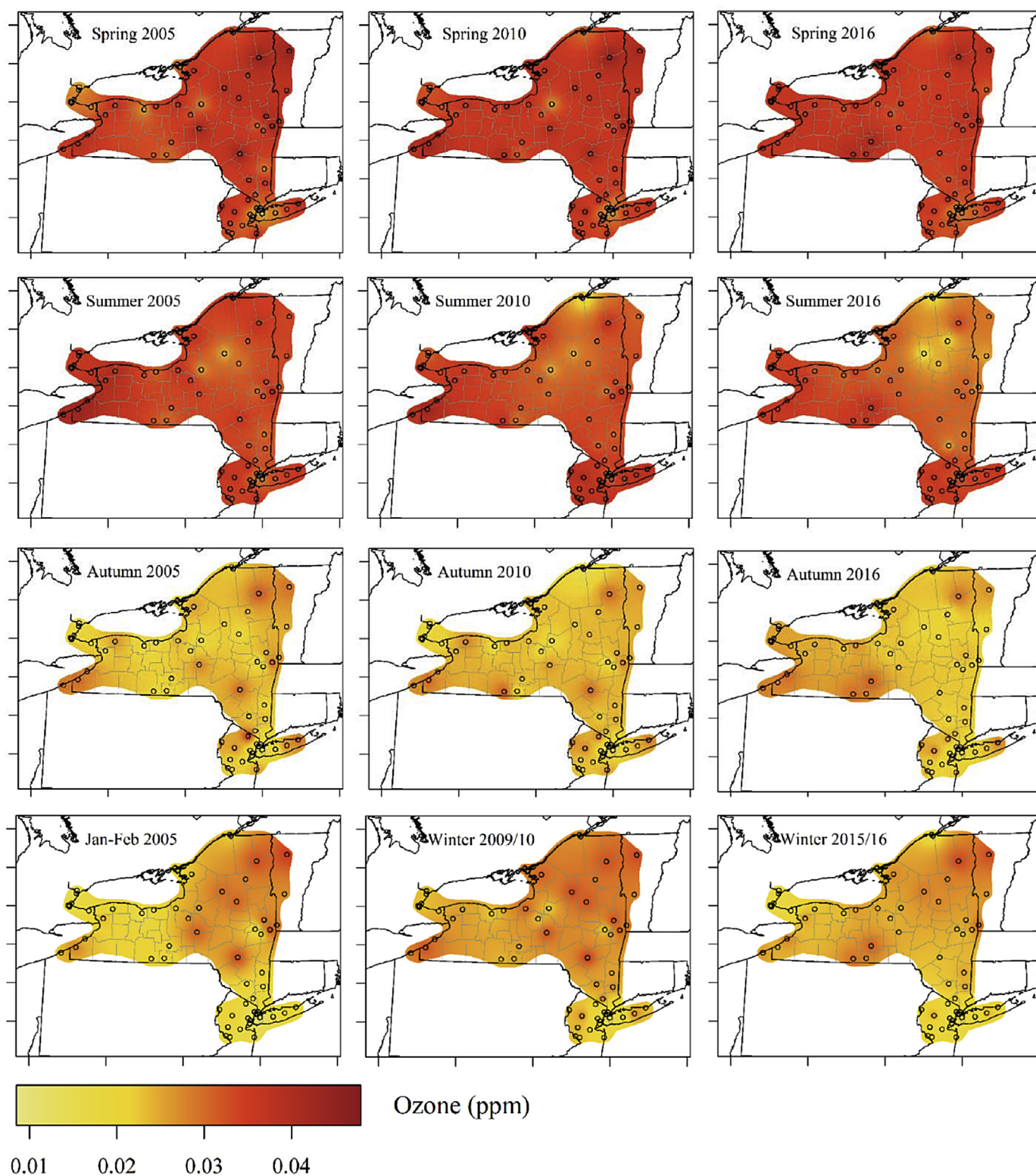


Fig. 7. Spatial interpolation of O₃ concentrations.

relationships between ambient concentration and estimated emissions ($r^2 > 0.8$). The highest decrease in CO concentrations was estimated at PFI, QUE and ROC ($-5.1\% \text{ y}^{-1}$, $-4.4\% \text{ y}^{-1}$ and $-4.3\% \text{ y}^{-1}$, respectively). LOU and BUF exhibited lower slopes ($-0.9\% \text{ y}^{-1}$). Good agreement between CO annual average concentrations and estimated emissions were obtained at PIN, LOU, PFI, QUE, and ROC. Unlike PM_{2.5}, NO_x and CO decrements did not show seasonal differences. NO_x

and CO emissions are mostly associated with highway vehicles and off-highway emissions (Figs. S3 and S4). During summer months, vehicular traffic increases (Fig. S23), but the higher mixing layer enhances dispersion. Conversely, winter months are characterized by lower vehicular traffic, but the lower mixing layer heights trap pollutants. Hence, the lack of marked seasonal differences in the slope reflects both the effects of differences in the mixing layer height and emissions among

Table 1

The statistics of the linear trends. Trends expressed in percentage (%) y^{-1} along with the upper and lower 95th confidence intervals in the trends and the p -values, which indicate the statistical significance of the slope estimation. Statistically significant trends are marked in bold (p -value < 0.05).

Site ID	Cat.	CO		NO _x		PM _{2.5}		SO ₂		O ₃	
		slope (l.ci, u.ci; p-value)% [start date - end date]	slope (l.ci, u.ci; p-value)% [start date - end date]	slope (l.ci, u.ci; p-value)% [start date - end date]	slope (l.ci, u.ci; p-value)% [start date - end date]	slope (l.ci, u.ci; p-value)% [start date - end date]	slope (l.ci, u.ci; p-value)% [start date - end date]	slope (l.ci, u.ci; p-value)% [start date - end date]	slope (l.ci, u.ci; p-value)% [start date - end date]	slope (l.ci, u.ci; p-value)% [start date - end date]	
AMH	SUB									0.9 (0.4, 1.5; 0) [1/1/2005 - 12/1/2016]	
TON	SUB							-6.2 (-6.8, -5.7; 0) [7/1/2007 - 12/1/2016]			
BUF	URB	-0.9 (-1.3, -0.5; 0) [1/1/2005 - 12/1/2016]	-5.4 (-5.8, -5; 0) [1/1/2005 - 12/1/2016]	-3.7 (-4.1, -3.1; 0) [1/1/2005 - 12/1/2016]				-5.7 (-6.2, -4.8; 0) [1/1/2005 - 12/1/2016]			
DUN	URB							-7.4 (-8.1, -6.7; 0) [1/1/2005 - 12/1/2016]			0.2 (-0.3, 0.6; 0.427) [1/1/2005 - 12/1/2016]
NIC	RUR							-2.1 (-2.8, -1.6; 0) [1/1/2005 - 12/1/2016]			-0.4 (-0.8, 0; 0.033) [1/1/2005 - 12/1/2016]
PIN	RUR		1.8 (-1, 6.1; 0.237) [6/1/2007 - 12/1/2016]		-3.4 (-4.1, -2.8; 0) [1/1/2005 - 12/1/2016]			-10.8 (-12, -9.7; 0) [1/1/2007 - 12/1/2016]			-0.4 (-1, 0.1; 0.13) [1/1/2006 - 11/1/2016]
SYR	SUB				-3.4 (-4.1, -2.7; 0) [1/1/2005 - 12/1/2016]			-4.4 (-5.1, -3.8; 0) [1/1/2005 - 12/1/2016]			0.7 (0.2, 1.3; 0.01) [4/1/2005 - 12/1/2016]
ROC	URB	-4.3 (-4.8, -4.1; 0) [1/1/2005 - 12/1/2016]			-3.4 (-3.9, -2.7; 0) [1/1/2005 - 12/1/2016]			-8.6 (-9.2, -8; 0) [1/1/2005 - 12/1/2016]			1.4 (0.7, 2.1; 0) [1/1/2005 - 12/1/2016]
PAU	RUR							-1.1 (-1.5, -0.8; 0) [1/1/2005 - 12/1/2016]			
PIS	RUR							-1.8 (-2.4, -1.4; 0) [1/1/2005 - 12/1/2016]			-0.6 (-1, -0.2; 0) [1/1/2005 - 12/1/2016]
WHF	RUR				-3.3 (-4.1, -2.2; 0) [1/1/2005 - 12/1/2016]			-1.6 (-2, -1.2; 0) [1/1/2005 - 12/1/2016]			0.1 (-0.2, 0.4; 0.391) [1/1/2005 - 12/1/2016]
Y001	RUR							-2.9 (-4.6, -0.2; 0.043) [1/1/2005 - 12/1/2016]			
STI	RUR										-0.5 (-0.9, -0.2; 0.007) [1/1/2005 - 12/1/2016]
LOU	SUB	-0.9 (-1.3, -0.6; 0) [1/1/2005 - 12/1/2016]			-2.9 (-4, -1.7; 0) [1/1/2008 - 12/1/2016]			-8.1 (-8.5, -7.4; 0) [1/1/2005 - 12/1/2016]			0.8 (0.4, 1.3; 0) [1/1/2005 - 12/1/2016]
ALB	URB				-3.8 (-4.4, -3.1; 0) [1/1/2005 - 12/1/2016]						
MIL	RUR										1.5 (0.9, 2.2; 0) [1/1/2005 - 12/1/2016]
MTN	RUR							-5.6 (-6.6, -4.7; 0) [1/1/2005 - 12/1/2016]			-0.1 (-0.5, 0.4; 0.825) [4/1/2005 - 12/1/2016]
BAB	SUB				-3.5 (-4.1, -2.9; 0) [1/1/2006 - 12/1/2016]						1.2 (0.6, 1.8; 0) [1/1/2005 - 12/1/2016]
EIS	SUB							-7.2 (-8, -6.5; 0) [1/1/2005 - 12/1/2016]			
HOL	SUB							-8 (-8.6, -7.5; 0) [1/1/2005 - 12/1/2016]			-0.2 (-0.7, 0.1; 0.18) [1/1/2005 - 12/1/2016]
JHS126	SUB				-4 (-4.5, -3.5; 0) [1/1/2005 - 12/1/2016]						
WHP	SUB										0.6 (0.2, 1; 0.01) [1/1/2005 - 12/1/2016]
CCNY	URB										3.2 (2.4, 4.1; 0) [7/1/2007 - 12/1/2016]
DIV	URB				-3.7 (-4.5, -2.8; 0) [3/1/2007 - 12/1/2016]						
IS52	URB		-4.3 (-4.8, -3.9; 0) [1/1/2005 - 12/1/2016]		-3.3 (-3.7, -2.5; 0) [1/1/2005 - 12/1/2016]			-8.8 (-9.5, -8.2; 0) [1/1/2005 - 12/1/2016]			3.5 (2.9, 4.2; 0) [1/1/2005 - 12/1/2016]
JHS45	URB				-4.2 (-4.6, -3.6; 0) [1/1/2005 - 12/1/2016]						
NEW	URB				-3.9 (-4.4, -3.2; 0) [1/1/2005 - 12/1/2016]						
PFI	URB	-5.1 (-5.8, -4.5; 0) [1/1/2007 - 12/1/2016]	-5 (-5.5, -4.6; 0) [1/1/2007 - 12/1/2016]		-2.2 (-3.2, -1.1; 0) [1/1/2008 - 12/1/2016]			-8.1 (-9.1, -7.4; 0) [2/1/2007 - 12/1/2016]			3.3 (2.5, 4; 0) [1/1/2007 - 12/1/2016]
POR	URB				-4.2 (-4.7, -3.6; 0) [1/1/2005 - 12/1/2016]						
PS19	URB				-3.4 (-3.9, -2.8; 0) [1/1/2005 - 12/1/2016]						
QUE	URB	-4.4 (-4.8, -3.8; 0) [1/1/2005 - 12/1/2016]	-4.2 (-4.4, -3.8; 0) [1/1/2005 - 12/1/2016]		-3.9 (-4.3, -3.3; 0) [1/1/2005 - 12/1/2016]			-8.5 (-9, -8; 0) [1/1/2005 - 12/1/2016]			2.7 (2.2, 3.2; 0) [1/1/2005 - 12/1/2016]

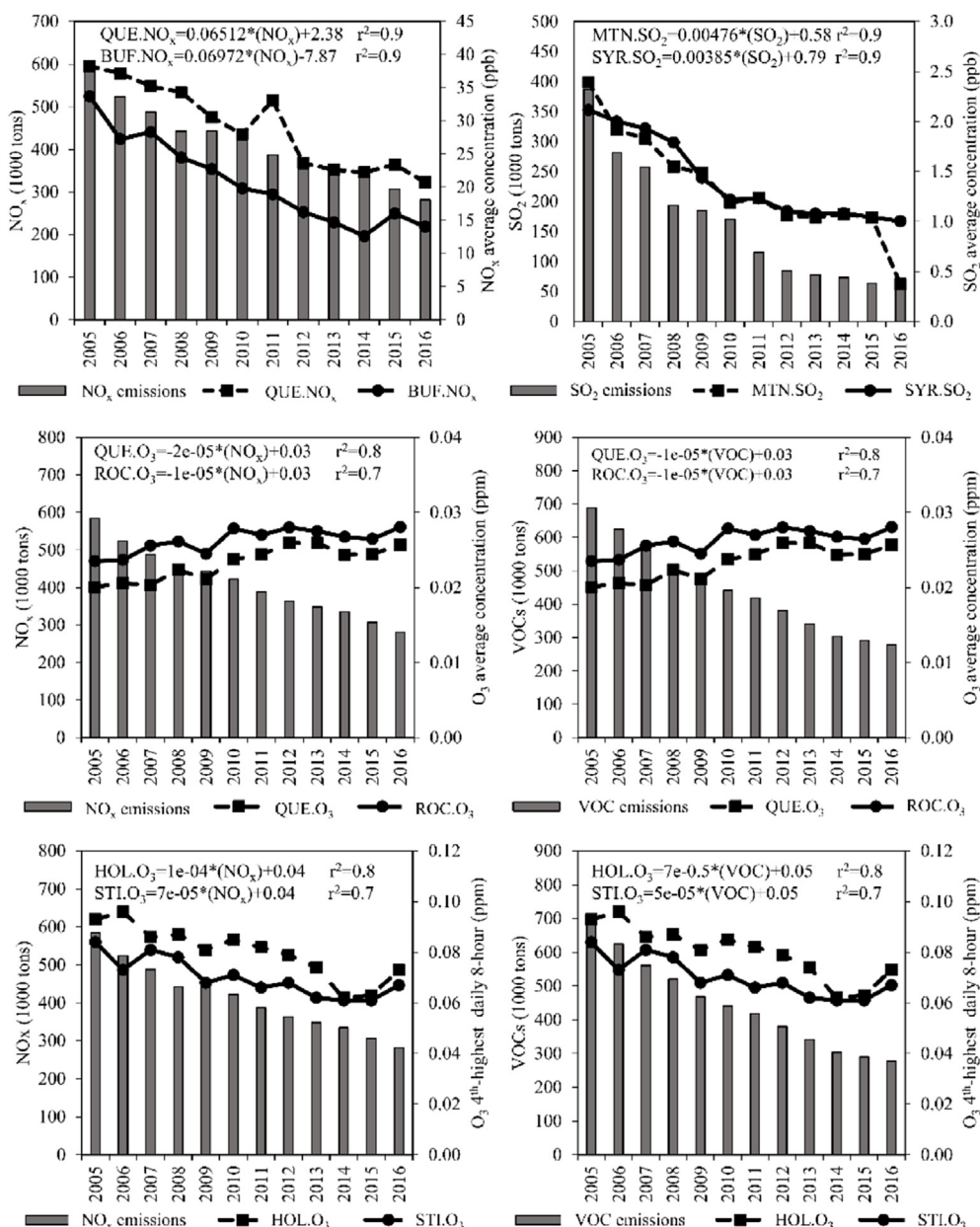


Fig. 8. Estimated emissions for NO_x, SO₂ and VOC (left axis), annual average ambient concentrations for NO_x, SO₂, O₃ and the O₃ annual 4th-highest daily maximum 8-h concentration (right axis), the reported equations are the linear regression model relating annual average ambient concentrations to the annual emissions.

the seasons.

Similar to NO_x, SO₂ concentrations dropped significantly at all sites in the 2005 to 2016 period, with the highest slopes observed at the urban sites (i.e., ROC -8.6% y⁻¹, IS52 -8.8% y⁻¹, QUE -8.5% y⁻¹). The smallest, but still significant slopes, were recorded at rural sites (NIC, -2.1%; PAU, -1.1% y⁻¹; WHF, -1.6% y⁻¹ and PIS, -1.8% y⁻¹). Significant direct relationships between ambient SO₂ and emissions were observed at all sites except TON, with R² > 0.8 at MTN, PAU, PIN, WHF, SYR, HOL, DUN, IS52, QUE, and ROC.

Seasonally, the rural sites showed the highest decreases during winter with values ranging from -3.8% y⁻¹ at NIC to -7.9% y⁻¹ at MTN. At these sites, it is likely that the main source of SO₂ is the combustion of oil for space heating rather than industrial or EGU emissions. Therefore, the reduction of SO₂ emissions can be related to transition to ultralow-sulfur No.2 oil imposed by New York State.

PIN, and the suburban and urban sites exhibited a different pattern with decreases for all seasons. At these sites, industrial and EGUs emissions might exceed space heating. The PIN site may be affected by

intensive fracking activities across the nearby border with Pennsylvania (State Impact PA, 2018) TON, BUF, and DUN can be affected by emissions from the Buffalo industrial area and from Hamilton and Burlington (CA). NYC sites (IS52, PFI and QUE) are affected by the emissions of the industrial, marine, and power plant facilities located in the Jersey City-Newark-Elisabeth area (Qin et al., 2006).

4.4.1. Ozone trends and relationship with NO_x and VOC

Despite the general decrease in NO_x concentrations and emissions across the state, decreases in O₃ concentrations at all sites were not observed. Throughout the period, ozone concentrations showed no significant trend at rural sites (MTN, PIN, and WHF), DUN and HOL (suburban). A statistically significant increase was estimated for urban and suburban sites with the highest slopes at the NYC sites (CCNY, +3.2% y⁻¹; IS52, +3.5% y⁻¹; PFI, +3.3% y⁻¹ and QUE, +2.7% y⁻¹). Only NIC, PIS, and STI (rural sites) exhibited a statistically significant decrease in ozone concentrations of -0.4% y⁻¹, -0.6% y⁻¹, and -0.5% y⁻¹, respectively. Seasonally, statistically significant

decreases in ozone concentrations were observed during summer at all rural sites except WIL, WHF, and MIL. SYR and DUN exhibited similar summer slopes ($-1.2\% \text{ y}^{-1}$ and $-1.5\% \text{ y}^{-1}$, respectively).

The reduction of NO_x emissions (-52%) likely contributed to the reduction of ozone formation during summer mostly at rural sites ($-1.9 \pm 0.4\% \text{ y}^{-1}$ on average). Similarly, NO_x and VOCs control plans successfully acted on the reduction of O_3 highest concentrations at rural and suburban sites. This conclusion is supported by the significant direct relationships between the O_3 annual 4th-highest daily maximum 8-h concentrations, i.e. the metric used by US EPA for the NAAQS O_3 standard, NO_x and VOCs emissions ($r^2 \sim 0.7$) (Fig. 8 and Table S10).

Conversely, the mitigation strategies did not contribute to the reduction of spring maxima and led to increased concentrations in autumn and winter months. During spring, most of the sites showed no statistically significant trends or significant positive slopes (e.g., $+2.6\% \text{ y}^{-1}$ and $+2\% \text{ y}^{-1}$, at CCNY and PFI, respectively). Increased ozone concentrations were observed during autumn and winter, mostly at urban and suburban sites, but also at WIL and MIL (rural). Unlike other sites, the NYC sites (IS52, PFI and QUE) exhibited statistically significant positive slopes in all seasons, with the highest increases during winter ($6.6 \pm 0.4\% \text{ y}^{-1}$ on average).

Similar behavior was reported by Austin et al. (2015) in the metropolitan Boston area. In the present study, increased background concentrations of ozone were observed mostly during the transition period (spring and falls) in agreement with increased spring maximal O_3 concentrations (Monks, 2000). Bloomer et al. (2010) and Simon et al. (2015) observed an increase in ozone concentrations at the lower end of the ozone distribution during winter and early spring months in more urbanized areas, probably because of decreased NO titration (Clifton et al., 2014).

The inverse relation between average measured O_3 and estimated NO_x can help explain the behavior of ozone in the urban sites (Fig. 8). Under VOC limited conditions (Seinfeld and Pandis, 2016), the reaction of $\cdot\text{OH}$ with NO_2 predominates over the reaction of $\cdot\text{OH}$ with VOCs, i.e., the effects of NO_x on ozone are dominated by ozone destruction. Thus, in areas characterized by elevated ambient NO_x concentrations (e.g., urban centers with significant traffic), ozone concentrations are controlled by VOC-limited conditions leading to ozone suppression. In these cases, NO_x reductions may lead to increased ozone concentrations and frequently violations of the NAAQS ozone standard at downwind suburban sites outside of core urban areas (Simon et al., 2015).

The failure of NO_x emissions reduction to reduce ozone concentrations can also be due in part to the addition of exhaust after-treatment systems in diesel vehicles leading to increases in the fraction of NO_2 in the NO_x emissions from traffic. The increased NO_2 can result in shifting in the photostationary state in favor of NO_2 without an equivalent decrease in O_3 concentrations (Guerreiro et al., 2014). At IS52, PFI, and QUE, the decrease in NO_x concentrations is larger than the decrease in NO_2 concentrations, resulting in a statistically significant increase in the NO_2/NO_x ratio (IS52 $+1.2\% \text{ y}^{-1}$; PFI $+1.0\% \text{ y}^{-1}$; QUE $+0.5\% \text{ y}^{-1}$) (Fig. S24).

4.5. Economy and air pollution

The ambient pollutant concentrations respond to emission changes, which in turn are driven by economic activity and emissions control regulations. Emission inventories represent a useful tool to understand the main changes in air pollutants emissions, but emissions are usually estimated on annual average basis. Conversely, some economic indicators are available at monthly scale potentially providing better insights on the economic impacts on air pollutants trends. Thus, the effects of economic changes on air pollution was evaluated by using some economic indicators as proxies for specific economic sectors. Ozone was not included in this analysis because it is a secondary pollutant. For each pollutant at each site, a multilinear regression model was

computed between the monthly average pollutant concentration and the monthly averages of the economic indicators for NYS. Energy sales for transportation and industry were used to characterize the associated variation in pollution concentrations from the transportation and industrial sector, respectively. The residential heating oil price was used to account for the changes in residential space heating fuels during the period. Gasoline prices might affect the overall traffic and the net electricity generation by coal and by natural gas characterizes the changes in electricity production fuels. Results of the multilinear regression are reported as supplementary materials (Tables S11 to S18).

The decrease in net electricity generation by coal affected $\text{PM}_{2.5}$ concentrations across the state (Tables S11 and S12) with statistically significant positive coefficients obtained at almost all sites (p -value < 0.05), i.e., the decrease of coal use led to an overall decrease of $\text{PM}_{2.5}$. Lower but statistically significant positive coefficients were obtained for the electricity generation by natural gas at most sites. Thus, the energy sector was a major driver for $\text{PM}_{2.5}$ concentrations. The industrial sector is positively related to $\text{PM}_{2.5}$ concentrations at WES, NIA, and BUF. The Buffalo area is one of the more industrialized areas of the state with several manufacturer industries (Buffalo Niagara, 2017). Statistically significant negative coefficients for residual oil were obtained only at WES, PIN, WHF, and NIA, while, LOU and PFI had positive coefficients.

SO_2 concentrations across the state were related to the trends in residual oil prices, electricity generation by coal, and electricity generation by natural gas (Tables S13 and S14). The decrease in coal combustion for electricity generation led to decreases in SO_2 concentration whereas natural gas generation had a negative coefficient, i.e. the shift from coal to natural gas produced negative SO_2 trends. Positive and statistically significant coefficients were obtained for industrial energy sales and for residual oil prices. An increase in industrial production led to increased SO_2 concentrations. The positive relationship between SO_2 and residual oil prices was unexpected. This pattern may be related to a seasonal effect, SO_2 average concentrations are higher during winter months and residual oil prices tend to increase during cold months which are also when there is more demand of oil for space heating and higher emissions.

The decrease in electricity generation by coal led to decreased NO_x concentrations similar to PM and SO_2 , (Tables S15 and S16). Changes in residual oil and gasoline prices affected NO_x concentration at all sites. Like the SO_2 results, positive coefficients for residual oil price in the NO_x models can be the result of season related to the increasing demand for residual oil for space heating and the subsequent emissions of NO_x . Gasoline price had a negative coefficient indicating a decrease in traffic volume and a subsequent decrease in NO_x concentrations.

CO concentrations were primarily related to the variations in generation by coal and by natural gas (Tables S17 and S18). Decreased generation by coal led to decreased CO concentrations. Additionally, increased energy generation with natural gas also reduced CO concentrations because of lower carbon monoxide emissions from natural gas combustion (EIA, 1999).

5. Conclusions

Over the past decade, mitigation strategies were implemented at both the federal and state levels in the United States (US) to reduce SO_2 and NO_x emissions from light- and heavy-duty vehicles and electric power generation. During this period, the US experienced one of the worst financial/economic crisis of the last century followed by a recession period. The combined effects of the mitigation strategies and the recession led to an overall decrease in $\text{PM}_{2.5}$ and primary gaseous pollutants concentrations across New York State ultimately resulting in relatively homogeneous spatial distributions for $\text{PM}_{2.5}$ and SO_2 . Ozone presented different seasonal patterns. Summer months showed decreases in ozone concentrations, mostly in the central and north part of the state while ozone increased during winter and spring leading to a less spatial variability. The reduction of NO_x emissions contributed to

the reduction of ozone formation during summer, but it did not reduce the spring maxima. NO_x reductions likely led to increases in autumn and winter ozone concentrations. The shift from coal to natural gas in electricity generation was the major driver of changes in pollutants concentrations across New York State. In the Buffalo area, one of the most industrialized areas of the state, changes in industrial production also affected PM_{2.5} and SO₂ concentrations. NO_x concentrations were also related to variations in gasoline prices. Thus, both mitigation strategies and economic factors can significantly affect air pollutant concentrations and trends in concentrations and emissions over time.

Acknowledgments

This work was supported by the New York State Energy Research and Development Authority (NYSERDA) under agreements #59800, 59802, and 100412.

Appendix A. Supplementary data

Supplementary data related to this article can be found at <http://dx.doi.org/10.1016/j.atmosenv.2018.03.045>.

References

- Arruti, A., Fernández-Olmo, I., Irabien, A., 2011. Impact of the global economic crisis on metal levels in particulate matter (PM) at an urban area in the Cantabria Region (Northern Spain). *Environ. Pollut.* 159, 1129–1135. <https://doi.org/10.1016/j.envpol.2011.02.008>.
- Austin, E., Zanobetti, A., Coull, B., Schwartz, J., Gold, D.R., Koutrakis, P., 2015. Ozone trends and their relationship to characteristic weather patterns. *J. Expo. Sci. Environ. Epidemiol.* 25, 532–542. <https://doi.org/10.1038/jes.2014.45>.
- Bigi, A., Harrison, R.M., 2010. Analysis of the air pollution climate at a central urban background site. *Atmos. Environ.* 44, 2004–2012. <https://doi.org/10.1016/j.atmosenv.2010.02.028>.
- Bloomer, B.J., Vinnikov, K.Y., Dickerson, R.R., 2010. Changes in seasonal and diurnal cycles of ozone and temperature in the eastern U.S. *Atmos. Environ.* 44, 2543–2551. <https://doi.org/10.1016/j.atmosenv.2010.04.031>.
- Buffalo Niagara, 2017. Major Employers. available at: <http://www.buffaloniagara.org/RESOURCES-MAPS/Major-Employers.aspx> accessed December 11, 2017.
- Carlsaw, D.C., 2017. Package “Openair”. Tools for the Analysis of Air Pollution Data. Available from: www.openair-project.org/ accessed September 23, 2017.
- Carlsaw, D.C., Ropkins, K., 2012. Openair - an R package for air quality data analysis. *Environ. Model. Software* 27–28, 52–61. <https://doi.org/10.1016/j.envsoft.2011.09.008>.
- Census, 2017a. United States Census Bureau, Quick Fact New York. available at: <https://www.census.gov/quickfacts/NY> (last access: December 2017).
- Census, 2017b. United States Census Bureau, State-based Metropolitan and Micropolitan Statistical Areas Maps. available at: <https://www.census.gov/geo/maps-data/maps/statecbsa.html> (last access: November 2017).
- Chan, E., Vet, R.J., 2010. Baseline levels and trends of ground level ozone in Canada and the United States. *Atmos. Chem. Phys.* 10, 8629–8647. <https://doi.org/10.5194/acp-10-8629-2010>.
- Civerolo, K.L., Rattigan, O.V., Felton, H.D., Schwab, J.J., 2017. Changes in gas-phase air pollutants across New York state, USA. *Aerosol Air Qual. Res.* 17, 147–166. <https://doi.org/10.4209/aaqr.2016.04.0141>.
- Cleveland, W.S., McRae, J.E., 1978. Weekday–weekend ozone concentrations in the Northeast United States. *Environ. Sci. Technol.* 12, 558–563.
- Cleveland, W.S., Graedel, T.E., Kleiner, B., Warner, J.L., 1974. Sunday and workday variations in photochemical air pollutants in New Jersey and New York. *Science* 186, 1037–1038.
- Clifton, O.E., Fiore, A.M., Correa, G., Horowitz, L.W., Naik, V., 2014. Twenty-first century reversal of the surface ozone seasonal cycle over the northeastern United States. *Geophys. Res. Lett.* 41, 7343–7350.
- DEC, 2017. 2017 ANNUAL MONITORING NETWORK PLAN - New York State Ambient Air Monitoring Program. Retrieved from: <http://www.dec.ny.gov/chemical/33276.html>.
- Di, Q., Dai, L., Wang, Y., Zanobetti, A., Choirat, C., Schwartz, J.D., Dominici, F., 2017. Association of short-term exposure to air pollution with mortality in older adults. *J. Am. Med. Assoc.* 318 (24), 2446–2456. <http://dx.doi.org/10.1001/jama.2017.17923>.
- Duncan, B.N., Lamsal, L.N., Thompson, A.M., Yoshida, Y., Lu, Z., Streets, D.G., Hurwitz, M.M., Pickering, K.E., 2016. A space-based, high-resolution view of notable changes in urban NO_x pollution around the world (2005–2014). *J. Geophys. Res. Atmos.* 121, 976–996. <https://doi.org/10.1002/2015JD024121>.
- Dutkiewicz, V.A., Qureshi, S., Khan, A.R., Ferraro, V., Schwab, J., Demerjian, K., Husain, L., 2004. Sources of fine particulate sulfate in New York. *Atmos. Environ.* 38, 3179–3189. <https://doi.org/10.1016/j.atmosenv.2004.03.029>.
- Dutkiewicz, V.A., Husain, L., Roychowdhury, U.K., Demerjian, K.L., 2011. Black carbon transport to a remote mountaintop in the northeastern US and relationship with other pollutants. *Atmos. Environ.* 45, 2110–2119. <https://doi.org/10.1016/j.atmosenv.2011.01.049>.
- EIA, 1999. Natural Gas 1998 Issues and Trends. Retrieved from: http://webapp1.dlib.indiana.edu/virtual_disk_library/index.cgi/4265704/FID1578/pdf/gas/056098.pdf.
- Emami, F., Masiol, M., Hopke, P.K., 2018. Air pollution at Rochester, NY: long-term trends and multivariate analysis of upwind SO₂ source impacts. *Sci. Total Environ.* 612, 1506–1515. <https://doi.org/10.1016/j.scitotenv.2017.09.026>.
- Fine, P.M., Sioutas, C., Solomon, P.A., 2008. Secondary particulate matter in the United States: insights from the Particulate Matter Supersites Program and related studies. *J. Air Waste Manag. Assoc.* 58, 234–253. <https://doi.org/10.3155/1047-3289.58.2.234>.
- Gao, Y., Fu, J.S., Drake, J.B., Lamarque, J.-F., Liu, Y., 2013. The impact of emission and climate change on ozone in the United States under representative concentration pathways (RCPs). *Atmos. Chem. Phys.* 13, 9607–9621.
- Guerreiro, C.B.B., Foltescu, V., de Leeuw, F., 2014. Air quality status and trends in Europe. *Atmos. Environ.* 98, 376–384. <https://doi.org/10.1016/j.atmosenv.2014.09.017>.
- Hand, J.L., Schichtel, B.A., Pitchford, M., Malm, W.C., Frank, N.H., 2012a. Seasonal composition of remote and urban fine particulate matter in the United States. *J. Geophys. Res. Atmos.* 117, 1–22. <https://doi.org/10.1029/2011JD017122>.
- Hand, J.L., Schichtel, B.A., Malm, W.C., Pitchford, M.L., 2012b. Particulate sulfate ion concentration and SO₂ emission trends in the United States from the early 1990s through 2010. *Atmos. Chem. Phys.* 12, 10353–10365. <https://doi.org/10.5194/acp-12-10353-2012>.
- Hidy, G.M., Blanchard, C.L., Baumann, K., Edgerton, E., Tanenbaum, S., Shaw, S., Walters, J., et al., 2014. Chemical climatology of the southeastern United States, 1999–2013. *Atmos. Chem. Phys.* 14, 11893–11914. <https://doi.org/10.5194/acp-14-11893-2014>.
- Hoek, G., Krishnan, R.M., Beelen, R., Peters, A., Ostro, B., Brunekreef, B., Kaufman, J.D., 2013. Long-term air pollution exposure and cardio-respiratory mortality: a review. *Environ. Health* 12 (43). <https://doi.org/10.1186/1476-069X-12-43>.
- Homer, C.G., Dewitz, J.A., Yang, L., Jin, S., Danielson, P., Xian, G., Coulston, J., Herold, N., Wickham, J., Megown, K., 2015. Completion of the 2011 National Land Cover Database for the conterminous United States-Representing a decade of land cover change information. *Photogramm. Eng. Rem. Sens.* 81, 345–354.
- Hystad, P., Setton, E., Cervantes, A., Poplawski, K., Deschenes, S., Brauer, M., van Donkelaar, A., Lamsal, L., Martin, R., Jerrett, M., Demers, P., 2011. Creating national air pollution models for population exposure assessment in Canada. *Environ. Health Perspect.* 119, 1123–1129. <https://doi.org/10.1289/ehp.1002976>.
- Jerrett, M., Burnett, R.T., Ito, K., Thurston, G., Krewski, D., Shi, Y., Calle, E., Thun, M., 2009. Long-term ozone exposure and mortality. *N. Engl. J. Med.* 360, 1085–1095. <https://doi.org/10.1056/NEJMoa0803894>.
- Keirbek, I., Haney, J., Douglas, S., Ito, K., Caputo Jr., S., Matte, T., 2014. The public health benefits of reducing fine particulate matter through conversion to cleaner heating fuels in New York City. *Environ. Sci. Technol.* 48, 13573–13582.
- Lebron, F., 1975. A comparison of weekend-weekday ozone and hydrocarbon concentrations in the Baltimore–Washington metropolitan area. *Atmos. Environ.* 9, 861–863.
- Loughlin, D.H., Dodder, R.S., 2014. Engineering economic assessment of whole-house residential wood heating in New York. *Biomass Bioenergy* 60, 79–87. <https://doi.org/10.1016/j.biombioe.2013.10.029>.
- Malm, W.C., Schichtel, B.A., Ames, R.B., Gebhart, K.A., 2002. A 10-year spatial and temporal trend of sulfate across the United States. *J. Geophys. Res.: Atmos.* 107 (D22), 4627. <https://doi.org/10.1029/2002JD002107>.
- Malm, W.C., Schichtel, B.A., Pitchford, M.L., Ashbaugh, L.L., Eldred, R.A., 2004. Spatial and monthly trends in speciated fine particle concentration in the United States. *J. Geophys. Res.: Atmos.* 109, D03306. <https://doi.org/10.1029/2003JD003739>.
- Masiol, M., Mallon, C.O.L.T.M., Haines, K.M., Utell, M.J., Hopke, P.K., 2016. Airborne dioxins, furans, and polycyclic aromatic hydrocarbons exposure to military personnel in Iraq. *J. Occup. Environ. Med.* 58, S22–S30. <http://dx.doi.org/10.1097/JOM.0000000000000771>.
- Masiol, M., Hopke, P.K., Felton, H.D., Frank, B.P., Rattigan, O.V., Wurth, M.J., LaDuke, G.H., 2017a. Analysis of major air pollutants and submicron particles in New York City and Long Island. *Atmos. Environ.* 148, 203–214. <https://doi.org/10.1016/j.atmosenv.2016.10.043>.
- Masiol, M., Hopke, P.K., Felton, H.D., Frank, B.P., Rattigan, O.V., Wurth, M.J., LaDuke, G.H., 2017b. Source apportionment of PM_{2.5} chemically speciated mass and particle number concentrations in New York City. *Atmos. Environ.* 148, 215–229. <https://doi.org/10.1016/j.atmosenv.2016.10.044>.
- Masiol, M., Squizzato, S., Formenton, G., Harrison, R.M., Agostinelli, C., 2017c. Air quality across a European hotspot: spatial gradients, seasonality, diurnal cycles and trends in the Veneto region, NE Italy. *Sci. Total Environ.* 576, 210–224. <https://doi.org/10.1016/j.scitotenv.2016.10.042>.
- Monks, P.S., 2000. A review of the observations and origins of the spring ozone maximum. *Atmos. Environ.* 34 (21), 3545–3561. [https://doi.org/10.1016/S1352-2310\(00\)00129-1](https://doi.org/10.1016/S1352-2310(00)00129-1).
- NAPS, 2017. National Air Pollution Surveillance Program. Canada Air Quality Data. available at: <http://maps-cartes.ec.gc.ca/mnsa-naps/data.aspx?lang=en> (accessed November, 2017).
- NEFI (New England Fuel Institute), 2014. State Sulfur Bioheat Requirement for No. 2 Heating Oil in the Northeast and Mid-Atlantic States. Available at: <https://nefi.com/news/docs/heating-oil-standards-chart.pdf>.
- NYC Cleanheat, 2018. <https://www.nycleanheat.org/>.
- NYSDOT, 2017. Downloadable Traffic Data. available at: <https://www.dot.ny.gov/divisions/engineering/technical-services/highway-data-services/hdsb> (Last access:

- October 2017).
- NYSERDA, 2006. Air Pollution in New York State – Ozone and Particulate Matter: a Primer. Retrieved from: file:///smdnas/phs/Home/squizzato/New%20York%20State%20Air%20Quality/Paper/Biblio/NYSERDA_2006%20PM-Ozone-Primer.pdf.
- NYSERDA, 2016. New York State Wood Heat Report: an Energy, Environmental, and Market Assessment Final Report. NYSERDA Report 15-26. Retrieved from: <https://www.nyscrda.ny.gov/-/media/Files/...Solar.../15-26-NYS-Wood-Heat-Report.pdf>.
- Ontario, 2017. Ontario's Long-term Energy Plan. website: <https://www.ontario.ca/page/ontarios-long-term-energy-plan> (last access: December, 2017).
- Parrish, D.D., Singh, H.B., Molina, L., Madronich, S., 2011. Air quality progress in North American megacities: a review. *Atmos. Environ.* 45, 7015–7025. <https://doi.org/10.1016/j.atmosenv.2011.09.039>.
- Parrish, D.D., Law, K.S., Staehelin, J., Derwent, R., Cooper, O.R., Tanimoto, H., Volz-Thomas, A., Gilge, S., Scheel, H.-E., Steinbacher, M., Chan, E., 2013. Lower tropospheric ozone at northern midlatitudes: changing seasonal cycle. *Geophys. Res. Lett.* 40, 1631–1636. <http://dx.doi.org/10.1002/grl.50303>.
- Pebesma, E., Graeler, B., 2017. Package “Gstat”. *Spatial and Spatio-temporal Geostatistical Modelling, Prediction and Simulation*.
- Qin, Y., Kim, E., Hopke, P.K., 2006. The concentrations and sources of PM_{2.5} in metropolitan New York city. *Atmos. Environ.* 40 (S2), 312–332. <https://doi.org/10.1016/j.atmosenv.2006.02.025>.
- R Core Team, 2017. R: a Language and Environment for Statistical Computing. R Foundation for Statistical Computing, Vienna, Austria URL: <https://www.R-project.org/>.
- Rattigan, O.V., Civerolo, K.L., Dirk Felton, H., Schwab, J.J., Demerjian, K.L., 2016. Long term trends in New York: PM_{2.5} mass and particle components. *Aerosol Air Qual. Res.* 16, 1191–1205. <https://doi.org/10.4209/aaqr.2015.05.0319>.
- RGGI, 2017. Regional greenhouse gas initiative an initiative of the northeast and mid-atlantic states of the U.S. In: *The Investment of RGGI Proceeds in 2015*, Retrieved from: https://www.rggi.org/docs/ProceedsReport/RGGI_Proceeds_Report_2015.pdf.
- Seinfeld, J.H., Pandis, S.N., 2016. *Atmospheric Chemistry and Physics: from Air Pollution to Climate Change*, third ed. John Wiley & Sons, Hoboken, NJ.
- Sen, P.K., 1968. Estimates of the regression coefficient based on Kendall's tau. *J. Am. Stat. Assoc.* 63, 1379–1389.
- Simon, H., Reff, A., Wells, B., Xing, J., Frank, N., 2015. Ozone trends across the United States over a period of decreasing NOx and VOC emissions. *Environ. Sci. Technol.* 49, 186–195. <https://doi.org/10.1021/es504514z>.
- State Impact Pa, 2018. <http://stateimpact.npr.org/pennsylvania/drilling>.
- Strode, S.A., Rodriguez, J.M., Logan, J.A., Cooper, O.R., Witte, J.C., Lamsal, L.N., Damon, M., Van Aartsen, B., Steenrod, S.D., Strahan, S.E., 2015. Trends and variability in surface ozone over the United States. *J. Geophys. Res. Atmos.* 120, 9020–9042.
- Tai, A.P.K., Mickley, L.J., Jacob, D.J., 2010. Correlations between fine particulate matter (PM_{2.5}) and meteorological variables in the United States: implications for the sensitivity of PM_{2.5} to climate change. *Atmos. Environ.* 44, 3976–3984. <https://doi.org/10.1016/j.atmosenv.2010.06.060>.
- Theil, H., 1992. *A Rank-invariant Method of Linear and Polynomial Regression Analysis*. Henri Theil's Contributions to Economics and Econometrics. Springer, pp. 345–381 1992.
- USEPA, 2016a. Heavy-duty Highway Compression-ignition Engines and Urban Buses: Exhaust Emission Standards. Office of Transportation and Air Quality EPA-420-B-16-018, March 2016. Retrieved from: <https://nepis.epa.gov/Exe/ZyPDF.cgi/P100SMQA.PDF?Dockey=P100SMQA.PDF>.
- USEPA, 2016b. Highway and Nonroad, Locomotive, and Marine (NRLM) Diesel Fuel Sulfur Standards. Office of Transportation and Air Quality EPA-420-B-16-1005, March 2016. Retrieved from: <https://nepis.epa.gov/Exe/ZyPDF.cgi?Dockey=P10009ZL.pdf>.
- USEPA, 2017a. Light-duty Vehicles, Light-duty Trucks, and Medium-duty Passenger Vehicles: Tier 2 Exhaust Emission Standards and Implementation. Office of Transportation and Air Quality EPA-420-B-17-028 September 2017 Schedule. Retrieved from: <https://nepis.epa.gov/Exe/ZyPDF.cgi/P100SMQA.PDF?Dockey=P100SMQA.PDF>.
- USEPA, 2017b. NOx Budget Trading Program. website: <https://www.epa.gov/airmarkets/nox-budget-trading-program> (accessed November 2017).
- USEPA, 2017c. Air Pollutant Emissions Trends Data. website: <https://www.epa.gov/air-emissions-inventories/air-pollutant-emissions-trends-data> (accessed November 2017).
- USEPA, 2017d. Air Data. Annual Summary Data. website: https://aqsdri.epa.gov/aqswb/aqstmp/airdata/download_files.html#Annual (access November 2017).
- Vingarzan, R., 2004. A review of surface ozone background levels and trends. *Atmos. Environ.* 38, 3431–3442. <http://dx.doi.org/10.1016/j.atmosenv.2004.03.030>.
- Wei, T., Simko, V., Levy, M., Xie, Y., Jin, Y., Zembla, J., 2017. Package “corrplot”. Visualization of a Correlation Matrix. Available from: <https://cran.r-project.org/web/packages/corrplot/index.html> Accessed September 2017.
- World Health Organization (WHO), Regional Office for Europe, 2013. Review of Evidence on Health Aspects of Air Pollution – REVIHAAP Project. Technical Report, Available from: http://www.euro.who.int/_data/assets/pdf_file/0004/193108/REVIHAAP-Final-technical-report-final-version.pdf accessed on December 21, 2017.
- Wu, J., Winer, A.M., Delfino, R.J., 2006. Exposure assessment of particulate matter air pollution before, during, and after the 2003 Southern California wildfires. *Atmos. Environ.* 40, 3333–3348. <https://doi.org/10.1016/j.atmosenv.2006.01.05>.